Electronic Supplementary Information for

Introducing DDEC6 Atomic Population Analysis: Part 2. Computed Results for a Wide Range of Periodic and Nonperiodic Materials

Nidia Gabaldon Limas and Thomas A. Manz*

Department of Chemical & Materials Engineering, New Mexico State University, Las Cruces, New Mexico, 88003-8001.

*E-mail: tmanz@nmsu.edu

Contents

S1. Additional tables for core electron binding energies

Table S1. Experimental Ti $2p_{3/2}$ core electron binding energies (eV) measured by X-ray photoelectron spectroscopy (XPS) and theoretically computed NACs. Compounds ordered from lowest to highest average binding energy.

solid	$2p_{3/2}$ binding energy (eV)[a]		ICSD code	Ti net atomic charge				
	lower limit	upper limit		Bader	CM5	DDEC3	DDEC6	HD
Ti	453.66	454.14	44872	0.00	0.00	0.00	0.00	0.00
TiB_2	454.14	454.50	78848	1.30	1.53	1.74	1.36	0.44
TiO	454.88	455.33	56612	1.50	0.87	2.16	1.29	0.35
TiN	455.66	456.00	105128	1.59	1.20	2.59	1.61	0.42
$BaTiO_3$	458.28	458.71	99737	2.13	1.42	2.55	2.20	0.72
$TiCl_4$	458.36	458.71	280981	1.90	0.95	1.27	1.45	0.56
$PbTiO_3$	458.43	458.78	165498	2.12	1.39	2.48	2.16	0.63
$CaTiO_3$	458.57	459.00	163662	2.01	1.48	2.61	2.26	0.75
$SrTiO_3$	458.57	459.00	[b]	2.09	1.45	2.64	2.26	0.72
TiO_2	458.64	459.33	39166	2.08	1.47	2.53	2.28	0.72

[a] XPS values from reference S1. [b] $SrTiO_3$ was geometry optimized using PBE.

Table S2. Experimental K-edge energy (eV) of molybdenum-containing compounds and average Mo NAC computed by various charge assignment methods. Compounds ordered from lowest to highest K-edge energy.

solid	K-edge energy(eV)[a]	ICSD code	average Mo net atomic charge				
			Bader[a]	CM5	DDEC3[a]	DDEC6	HD
Mo	20005.3	41513 (*Fm-3m*)	0	0	0	0	0
MoS_2	20006.5	43560 (*R*3*mH*), 95570 (*P*63/*mmc*)	1.09, 1.09	0.75, 0.71	0.23, 0.21	0.58, 0.53	0.26, 0.25
Mo_2C	20006.9	43322 (*Pbcn*)	0.66	0.39	0.57	0.44	0.19
MoO_2	20011.0	152316 (*P*121/*c*1)	1.88	1.21	1.78	1.65	0.58
Rb_2MoO_4	20013.5	24904 (*C*12/*m*1)	2.13	1.36	2.12	1.92	0.80
MoO_3	20013.7	151751 (*Pnma*), 152312 (*Pbnm*)	2.36, 2.29	1.62, 1.63	2.38, 2.36	2.27, 2.23	0.82, 0.80

[a] From reference S2.

S2. Systems comprised almost entirely of surface atoms

Figure S1 compares DDEC6 to DDEC3 NACs for the same materials comprised almost entirely of surface atoms that were previously used by Manz and Sholl to prepare a similar plot comparing DDEC/c2 to DDEC3 NACs.[S3] We used the same geometries and electron density files as reference S3. These materials were: (a) B_4N_4 cluster, (b) BN nanotube, (c) hexagonal-BN sheet, (d) formamide (PW91 exchange-correlation functional with 6-311++G** and planewave basis

sets), (e) the metal-organic frameworks IRMOF-1 (DFT-optimized and X-ray diffraction geometries), MIL-53(Al), ZIF-90, ZIF-8, Zn-nicotinate (PW91 optimized geometry), and CuBTC, (f) $ZrN_4C_{52}H_{72}$ organometallic complex, (g) $ZrO_4N_4C_{52}H_{72}$ organometallic complex, (h) $[GdI]^{+2}$ (SDD and planewave basis sets), (i) the MgI, MoI, SnI, TeI, and TiI molecules using both SDD and planewave basis sets, (j) $[Cr(CN)_6]^{3-}$, (k) the ozone singlet and triplet spin states using the PW91, B3LYP, CCSD, SAC-CI, and CAS-SCF exchange-correlation theories, (l) ozone +1 cation doublet (PW91, B3LYP, and CCSD methods), (m) the $Fe_4O_{12}N_4C_{40}H_{52}$ noncollinear single molecule magnet, and (n) $[Cu_2N_{10}C_{36}H_{52}]^{2+}$ spin triplet. As shown in Figure S1, the DDEC6 NACs follow a trend similar to the DDEC3 NACs for materials comprised almost entirely of surface atoms, but the two charge measures provide statistically significant differences.

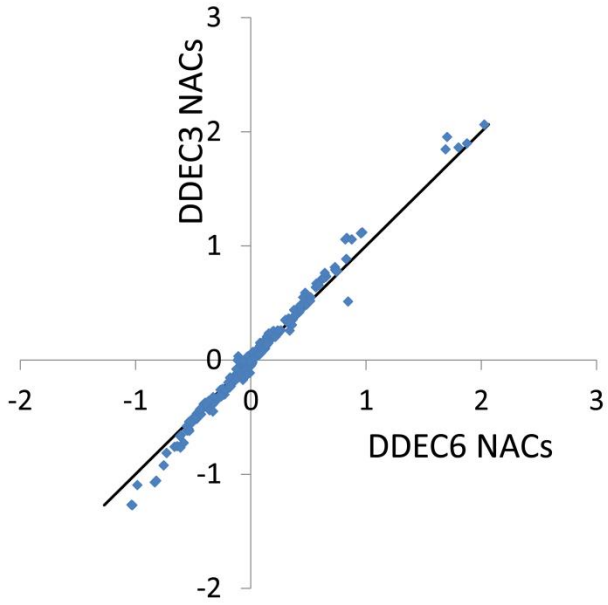

Figure S1. Comparison of DDEC3 and DDEC6 NACs for systems comprised almost entirely of surface atoms. The black line has a slope of 1 and an intercept of 0.

S3. Solid surfaces

A general purpose method for assigning NACs should yield reasonable results for both surface and buried atoms. This is significant, because some methods for assigning NACs such as DDEC/c1, DDEC/c2, ISA, REPEAT, ESP, etc. do not work well for buried atoms.[S3-S7] Here, we show the DDEC6 method continues to give reasonable results for three solid surfaces already studied with the DDEC3 method: a K adatom on a Mo_2C (110) surface, the NaF(001) surface, and the $SrTiO_3$(100) surface.[S3] The K adatom on a Mo_2C (110) surface slab geometry is from Han et al.,[S8] and for this material we used the same PBE-generated electron distribution and DDEC3 NACs as Manz and Sholl[S3]. We optimized the NaF(001) and $SrTiO_3$(100) surface slab geometries and electron distributions using the PBE functional at the PBE-optimized NaF and $SrTiO_3$ bulk lattice constants and used these to compute DDEC3 and DDEC6 NACs.

Figure S2 shows the geometries of these three surface slabs and compares the DDEC6 and DDEC3 NACs. For all three materials, the general trends displayed by the DDEC6 and DDEC3 NACs were similar, except the DDEC3 NACs were larger in magnitude than the DDEC6 NACs.

For all three of these solid surfaces, the DDEC6 method gave similar (but not identical) NACs for the surface and buried atoms of the same element.

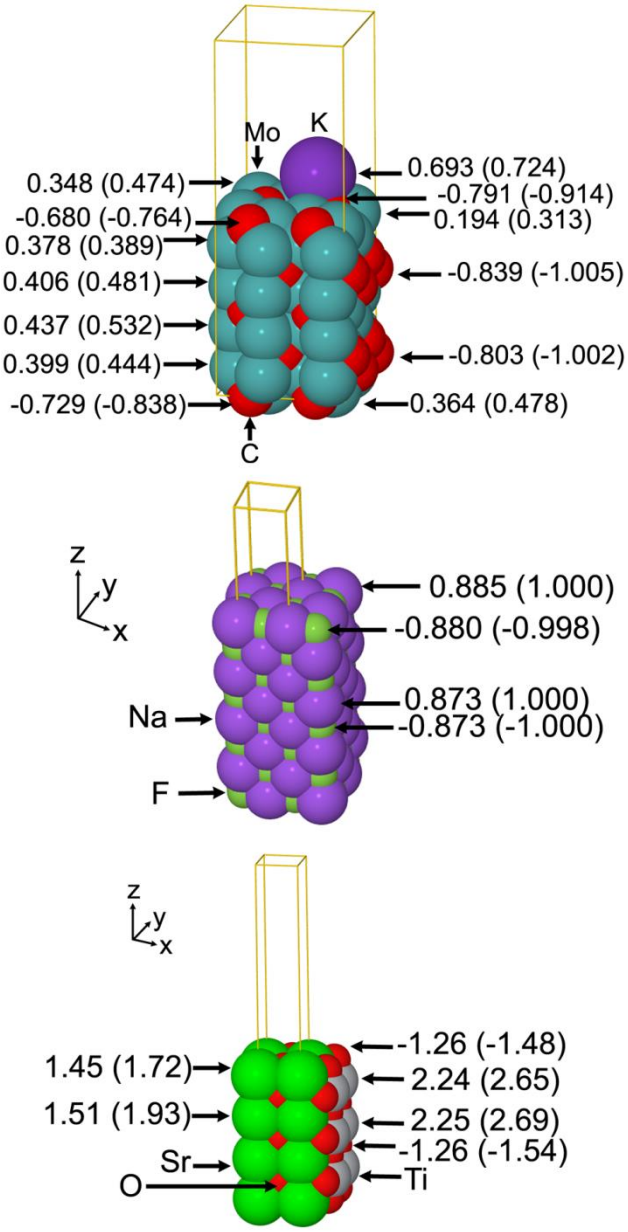

Figure S2. DDEC6 (and DDEC3 in parentheses) NACs of *top:* K adatom on a Mo_2C (110) surface; *center:* NaF(001) slab; *bottom:* $SrTiO_3$(100) slab.

Table S3 compares the NACs and atomic multipoles for the $SrTiO_3$ slab to those of the bulk material. $SrTiO_3$ is comprised of alternating SrO and TiO_2 layers. The trends in atomic dipoles were similar for the DDEC3 and DDEC6 methods. All of the atomic dipoles in the bulk material were zero due to symmetry. In the surface slab, each atom had a non-zero atomic dipole parallel to the direction of the surface normal. In both the bulk and slab materials, the $Q_{x^2-y^2}$ quadrupolar

component was zero for all atoms except the O atoms in the TiO_2 planes. Half the oxygen atoms in each TiO_2 plane had a positive value for the $Q_{x^2-y^2}$ quadrupolar component and the other half had a negative value. Because the surface breaks the crystal symmetry along the z-axis, the Sr and Ti atoms, which had $Q_{3z^2-r^2}=0$ in the bulk material, acquired non-zero $Q_{3z^2-r^2}$ moments in the surface slab. As shown in Table S3, the nonzero atomic multipole magnitudes were slightly higher for the surface atoms and decreased towards the bulk values as one moved towards the center of the slab.

Table S4 and Table S5 compare DDEC3, DDEC6, Bader, and IH/R3 NACs for bulk $SrTiO_3$ and NaF, respectively. We used PBE optimized geometries and electron distributions to compute the DDEC3, DDEC6, and Bader results. For these materials, the NAC magnitudes followed the trend DDEC3, IH/R3 > DDEC6, Bader.

Table S3. DDEC6 NACs and atomic multipole moments (in a.u.) for $SrTiO_3$(100) slab and bulk $SrTiO_3$.[a] DDEC3 NACs and atomic multipole moments shown in parentheses. Layer 1 is a surface layer, and layer 4 is in the middle of the slab.

Layer	Atom	NAC	μ_z	$Q_{x^2-y^2}$	$Q_{3z^2-r^2}$
1	O	-1.260 (-1.479)	0.111 (0.193)	0.000 (0.000)	-0.302 (-0.083)
1	Sr	1.443 (1.722)	-0.050 (-0.154)	0.000 (0.000)	0.349 (0.003)
2	O	-1.266 (-1.534)	-0.036 (-0.039)	±0.145 (±0.254)	0.107 (0.183)
2	Ti	2.236 (2.648)	-0.007 (-0.010)	0.000 (0.000)	-0.065 (-0.075)
3	O	-1.253 (-1.534)	0.020 (0.027)	0.000 (0.000)	-0.265 (-0.435)
3	Sr	1.505 (1.932)	0.005 (-0.018)	0.000 (0.000)	0.018 (0.009)
4	O	-1.265 (-1.562)	0.002 (0.001)	±0.143 (±0.245)	0.128 (0.213)
4	Ti	2.253 (2.686)	0.001 (-0.002)	0.000 (0.000)	-0.021 (-0.022)
Bulk	O (Sr)	-1.250 (-1.541)	0.000 (0.000)	0.000 (0.000)	-0.287 (-0.474)
Bulk	O (Ti)	-1.250 (-1.541)	0.000 (0.000)	±0.144 (±0.237)	0.144 (0.237)
Bulk	Sr	1.488 (1.927)	0.000 (0.000)	0.000 (0.000)	0.000 (0.000)
Bulk	Ti	2.262 (2.696)	0.000 (0.000)	0.000 (0.000)	0.000 (0.000)

[a] For all atoms, $\mu_x = \mu_y = Q_{xy} = Q_{xz} = Q_{yz} = 0.000$.

Table S4. NACs for $SrTiO_3$ crystal at ambient pressure. Results shown using the following number of frozen core electrons: Ti (12), Sr (28), and O (2).

Atom type	DDEC3	DDEC6	Bader	IH/R3[a]
O	-1.541	-1.250	-1.162	-1.43
Ti	2.696	2.262	2.091	2.69
Sr	1.927	1.488	1.394	1.62

[a] IH results from reference S9 using the R3 reference ions.

Table S5. NACs for NaF crystal at ambient pressure.

Atom type	DDEC3[a]	DDEC6[a]	Bader[a]	IH/R3[b]
Na	1.014 (1.000)	0.853 (0.877)	0.855 (0.798)	1.05
F	-1.014 (-1.000)	-0.853 (-0.877)	-0.855 (-0.798)	-1.05

[a] Values listed for 2 frozen Na core electrons; values in parenthesis for 10 frozen Na core electrons. [b] IH results from reference S9 using the R3 reference ions.

References:

S1. J. F. Moulder, W. F. Stickle, P. E. Sobol and K. D. Bomben, *Handbook of X-ray Photoelectron Spectroscopy*, ULVAC-PHI Inc., Chigasaki, Japan, 1995, pp. 1-261.

S2. L. W. Li, M. R. Morrill, H. Shou, D. G. Barton, D. Ferrari, R. J. Davis, P. K. Agrawal, C. W. Jones and D. S. Sholl, *J. Phys. Chem. C*, 2013, **117**, 2769-2773.

S3. T. A. Manz and D. S. Sholl, *J. Chem. Theory Comput.*, 2012, **8**, 2844-2867.

S4. T. A. Manz and D. S. Sholl, *J. Chem. Theory Comput.*, 2010, **6**, 2455-2468.

S5. P. Bultinck, D. L. Cooper and D. Van Neck, *Phys. Chem. Chem. Phys.*, 2009, **11**, 3424-3429.

S6. C. I. Bayly, P. Cieplak, W. D. Cornell and P. A. Kollman, *J. Phys. Chem.*, 1993, **97**, 10269-10280.

S7. T. Watanabe, T. A. Manz and D. S. Sholl, *J. Phys. Chem. C*, 2011, **115**, 4824-4836.

S8. J. W. Han, L. W. Li and D. S. Sholl, *J. Phys. Chem. C*, 2011, **115**, 6870-6876.

S9. D. E. P. Vanpoucke, I. Van Driessche and P. Bultinck, *J. Comput. Chem.*, 2013, **34**, 422-427.